Alignment of Ge Nanoislands on Si(111) by Ga-Induced Substrate Self-Patterning

Th. Schmidt,[1] J. I. Flege,[1] S. Gangopadhyay,[1] T. Clausen,[1] A. Locatelli,[2] S. Heun,[2,*] and J. Falta[1]

[1]*Institute of Solid State Physics, University of Bremen, Otto-Hahn-Allee 1, 28359 Bremen, Germany*

[2]*ELETTRA Synchrotron Light Source, Strada Statale 14, 34012 Basovizza, Italy*

(Received 22 September 2006; published 9 February 2007)

A novel mechanism is described which enables the selective formation of three-dimensional Ge islands. Submonolayer adsorption of Ga on Si(111) at high temperature leads to a self-organized two-dimensional pattern formation by separation of the 7×7 substrate and Ga/Si(111)-$(\sqrt{3} \times \sqrt{3}) - R30°$ domains. The latter evolve at step edges and domain boundaries of the initial substrate reconstruction. Subsequent Ge deposition results in the growth of 3D islands which are aligned at the boundaries between bare and Ga-covered domains. This result is explained in terms of preferential nucleation conditions due to a modulation of the surface chemical potential.

DOI: 10.1103/PhysRevLett.98.066104 PACS numbers: 68.35.−p, 68.37.Nq, 68.43.Jk, 68.65.Hb

Nanoscale three-dimensional Ge islands on Si substrates are of great interest, mainly due to their potential for optoelectronic applications [1,2]. A variety of approaches has been used in order to improve the uniformity and correlation of such islands. Most of them rely on prepatterning of the Si substrates. Artificial structures can be formed, e.g., by direct manipulation via an atomic force microprobe [3] or by conventional electron beam lithography and reactive ion etching processes [4,5]. Although these techniques offer precise control and alignment of Ge islands, they are hardly scalable. In this respect, self-organizing processes are more promising. In most cases, self-organized alignment is achieved by a strain modulation of the substrate. This can be obtained by deposition of coherent $Si_{1-x}Ge_x$ layers, which due to growth instabilities exhibit a surface undulation [6]. Alternatively, incoherent, i.e., dislocated $Si_{1-x}Ge_x$ layers grown on Si(001) can be used [7]. A third approach exploits the interaction of vertically stacked layers of GeSi clusters, which leads to a vertical alignment of these clusters, and through a self-organized ordering process [8] improves the lateral alignment and size distribution in the upper layers [9]. In all these cases, a periodic strain modulation of the substrate offers energetically preferential sites for Ge island nucleation and thus promotes island alignment. Surface energetics can also lead to an ordered growth of Ge islands, as has been observed on spontaneously faceted surfaces which can be obtained after Si buffer layer growth on vicinal Si(001) surfaces [10].

As far as ordering effects are concerned, less attention has been paid to the influence of surface kinetics. However, it is well known that smaller islands with higher density can be achieved when using Sb as a surfactant [11,12], which is known to reduce the effective surface diffusion of Ge [13]. Alternatively, submonolayer preadsorption of carbon, which induces a c-(4×4) reconstruction on Si(001) [14], can be used [15,16] to grow very small Ge islands at densities as high as 10^{11} cm^{-3}.

The adsorption of Ga on Si(111) is of specific interest, because it has been shown that, depending on Ga coverage, it can sharpen the island size distribution during subsequent Ge epitaxy [17]. In the present Letter, we show that a modulation of the surface properties by submonolayer adsorption of Ga can be used as a very promising alternative mechanism for Ge island alignment. In comparison to strain-based 3D island growth techniques, the approach presented here is expected to leave more freedom to tune the system's electronic properties, as will be explained below.

The experiments described in the following were carried out with the spectroscopic photoemission and low-energy electron microscope (SPELEEM) at the Nanospectroscopy beamline at ELETTRA [18,19]. Substrates were cut from highly oriented Si(111) wafers with a miscut angle below 0.02°. After degassing the substrates for at least 12 hours at 600 °C, a clean 7×7 surface reconstruction was prepared by 2–3 short flashes to 1200 °C for up to 30 seconds. Ga and Ge were evaporated from effusion cells operated by electron beam heating. First, Ga was deposited at a sample temperature slightly below the Ga redesorption threshold (at approximately 650 °C), i.e., very close to thermodynamic equilibrium conditions. Immediately after the Ga deposition, the substrate temperature was decreased in order to prevent Ga desorption. Subsequently, Ge was evaporated at 450 °C, without simultaneous supply of Ga. All deposition processes were monitored by LEEM in real time. The temperatures given here are estimated from the reading of a thermocouple attached at the sample holder. The thermocouple was calibrated to the Si(111)-(1×1) to Si(111)-(7×7) phase transition at about 830 °C.

The adsorption of Ga proceeds as shown in Fig. 1. The electron energy for these LEEM images was chosen in order to maximize the contrast at later stages of the experiment. Therefore, only a faint contrast is visible from the bare Si(111)-7×7 surface at the beginning. This contrast originates from step edges and domain boundaries of the 7×7 reconstruction. In Fig. 1 the step edges are oriented from the bottom towards the top of the images, and the domain boundaries of the 7×7 reconstruction are

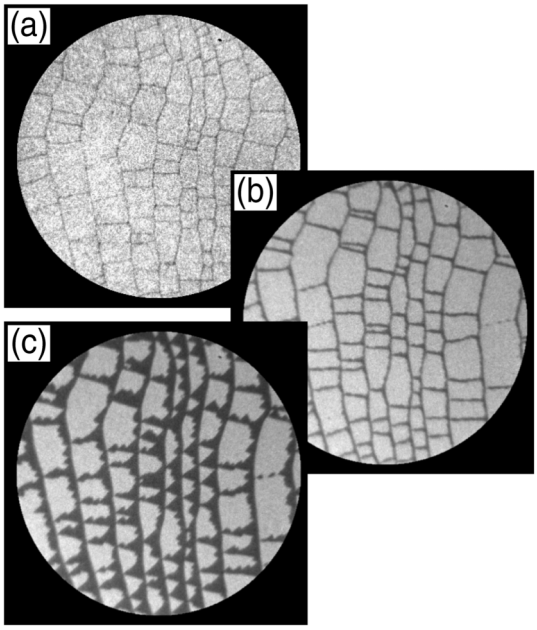

FIG. 1. Bright-field LEEM images of Si(111) during Ga deposition at about 650 °C. (Field of view: 5 μm, $E = 3.1$ eV). Step edges run bottom up; domain boundaries of the initial 7×7 run from left to right. (a) Prior to Ga deposition ($\Theta_{Ga} = 0$ ML), (b) nucleation of Ga $\sqrt{3}$ domains (dark) at step edges and 7×7 domain boundaries ($\Theta_{Ga} = 0.08$ ML), and (c) later stage of the nanopattern development after further Ga deposition ($\Theta_{Ga} = 0.13$ ML). [For display reasons, the gray scale contrast in (a) has been enhanced by a factor of 3 with respect to (b) and (c).]

approximately perpendicular to this direction. After the start of Ga deposition, a dark contrast arises both at step edges as well as at domain boundaries, as can be seen from Fig. 1(b) at a Ga coverage of $\Theta_{Ga} = 0.08$ ML. (1 ML = 7.83×10^{14} atoms/cm^2). As will be shown below, this is due to the nucleation of Ga/Si(111) $-$ $(\sqrt{3} \times \sqrt{3}) - R30°$ domains, which have a *local* coverage of 1/3 ML. With increasing Ga coverage the $\sqrt{3} \times \sqrt{3}$-$R30°$ (henceforth simply referred to as $\sqrt{3}$) patches grow in size. In Fig. 1(c), at $\Theta_{Ga} = 0.13$ ML, the typical shape of the $\sqrt{3}$ domains becomes visible, which reflects the threefold symmetry of the system. Since no nucleation at the interior of the 7×7 domains takes place, a two-dimensional phase separation results, and a nanopattern is achieved when the Ga deposition is stopped before the $\sqrt{3}$ reconstruction extends over the whole surface. The domain shape of the nanopattern is found to depend on the miscut orientation of the substrate. This observation and the underlying mechanisms are discussed in detail elsewhere [20].

A low-energy electron diffraction (LEED) pattern of the surface shown in Fig. 1(c) is presented in Fig. 2(a). It clearly reveals the coexistence of 7×7 and $\sqrt{3} \times \sqrt{3}$-$R30°$ reconstructed areas on the surface. A dark-field LEEM image obtained using one of the $\sqrt{3}$ superstructure spots is shown in Fig. 2(b). This unambiguously confirms

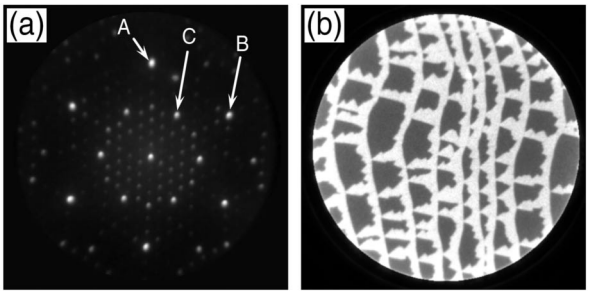

FIG. 2. Ga/Si(111) nanopattern after preparation. (a) LEED pattern ($E = 26$ eV) showing both 7×7 and $\sqrt{3}$ periodicity of the surface. First order spots (A and B) and a $\sqrt{3}$ superstructure spot (C) are labeled. (b) Dark-field LEEM image ($E = 28$ eV, 5 μm field of view). The $\sqrt{3}$ superstructure indicated in (a) was selected for this dark-field image. Areas with $\sqrt{3}$ periodicity therefore appear bright.

that $\sqrt{3}$ domains have formed at step edges and domain boundaries of the initial 7×7 reconstruction.

The evolution of the surface structure and morphology during Ge deposition onto a Ga/Si(111) nanopattern, as described above, is depicted in Fig. 3. In Fig. 3(a), after deposition of 0.3 ML Ge, the surface has already undergone a transformation. This can directly be seen from the drastic change in contrast [as compared to Fig. 1(c) which was obtained at the same electron energy]. Moreover, in an experiment which was performed under the same preparation conditions, the growth of Ge was interrupted in a stage comparable to that of Fig. 3(a), and with LEED, only a diffuse 7×7 pattern is found [cf. Fig. 3(b)]. That means, the previously observed $\sqrt{3}$ contributions [cf. Fig. 2(a)] have already vanished at the initial Ge growth stages. This indicates that Ge is incorporated preferentially at the former $\sqrt{3}$ patches, which leads to a site exchange of Ge and Ga, and thus to the transition from a Ga/Si(111)-$\sqrt{3}$ reconstruction to a Ga/Ge/Si(111)-(6.3×6.3) structure [21]. This incommensurate structure has a larger local Ga coverage as compared to Ga/Si(111)-$\sqrt{3}$. Since there is no further Ga supply from the gas phase, this leads to the formation of a patchwork of 6.3×6.3 Ga-terminated domains as well as Ga-depleted areas in between [21]. In the LEEM image in Fig. 3(a), the spotty appearance of the former $\sqrt{3}$ regions is a further indication for such a patchwork with a length scale near the resolution limit of the microscope.

Upon further Ge deposition, the contrast becomes weaker [see Figs. 3(c) and 3(d)], which can be attributed to a high density of mobile Ge adsorbate atoms on the surface [22]. In Fig. 3(e), small bright spots appear which are identified as Ge islands as will be shown below. The nucleation of these Ge islands is almost complete in Fig. 3(f), and the contrast in the image increases again. This points to a lattice relaxation of the islands which makes them stable against decay and energetically attractive to Ge adatoms [23], leading to a reduced adatom

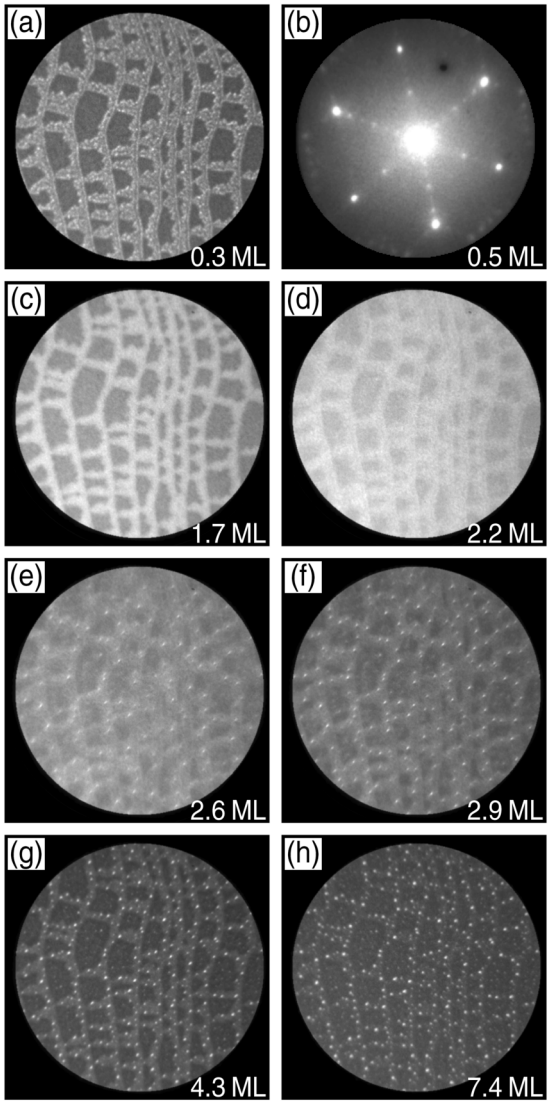

FIG. 3. (a) and (c)–(h) Bright-field LEEM images taken during Ge deposition at about 450 °C onto the surface shown in Fig. 1(c). (Field of view: 5 μm, $E = 3.1$ eV). The Ge deposit is indicated in each image. (b) LEED pattern after growth interruption obtained in an experiment performed under nearly identical conditions.

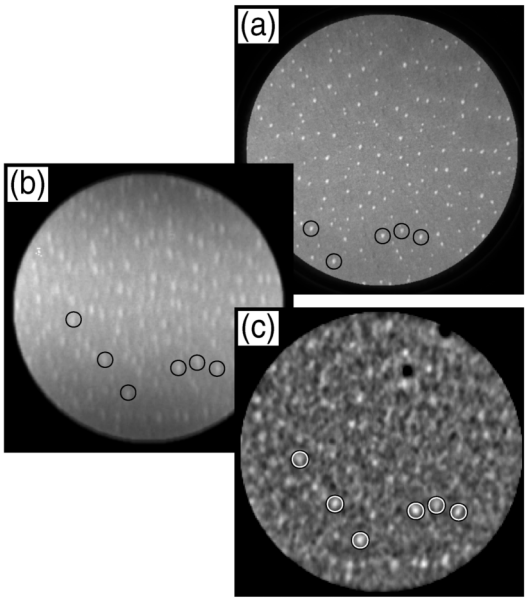

FIG. 4. Images taken after Ge deposition (5 μm field of view). (a) Bright-field LEEM ($E = 4.9$ eV), (b) XPEEM using Ge $3d$ photoelectrons ($E_{\mathrm{kin}} = 97.7$ eV, taken at about 120 eV photon energy; the elongated island shape is caused by sample drift). (c) XPEEM recorded with Ga $3d$ photoelectrons ($E_{\mathrm{kin}} = 107.7$ eV). All images show the same area on the surface. The circles mark identical objects.

density and thus to an enhanced image contrast [22]. From Figs. 3(f)–3(h), the number of islands remains almost constant and the lateral size of the islands increases only slightly, which indicates a three-dimensional island growth.

In order to unambiguously determine the nature of the bright spots referred to as Ge islands so far, a LEEM micrograph is compared to an x-ray photoemission electron micrograph (XPEEM) in Fig. 4(a) and 4(b). The image shown in Fig. 4(b) was obtained using Ge $3d$ photoelectrons and therefore directly provides chemical contrast. Taking a slight drift between the two images into account (see black circles), virtually every bright spot in the LEEM image can be identified as a Ge-rich region. This proves that the spots observed in LEEM indeed are Ge islands. The rather weak overall contrast of the XPEEM image in Fig. 4(b) is attributed to the existence of a Ge wetting layer between the islands. Upon closer inspection, a systematic dark shadow is visible in the right-hand side of these islands. Since the sample is illuminated from the left-hand side under an incident angle of 16° with respect to the surface, this dark contrast reveals the three-dimensional nature of the islands: at a photon energy of 120 eV, the attenuation length in Ge is about 30 nm, which is in the order of the lateral dimension of the Ge islands (about 50 nm FWHM). Hence the dark contrast is identified as a shadowing effect.

When comparing the XPEEM images in Fig. 4(b) and 4(c), a clear correlation between the Ge 3D islands and Ga-rich regions is revealed. Because of the surface sensitivity of the photoemission signal, this shows that Ga resides at the surface of the Ge 3D islands. Since it is rather unlikely that Ge 3D islands nucleate on Ga-free areas and Ga diffuses towards these islands afterwards, we conclude that the nucleation of such islands in Ga-rich regions is energetically favored as compared to nucleation on Ga-depleted areas, and Ga segregates to the surface during Ge 3D island growth. This conclusion is also supported by previous ion scattering and x-ray standing waves results [17,21] which have shown that Ga acts as a surfactant and segregates to the surface during Ge film growth. Hence, the

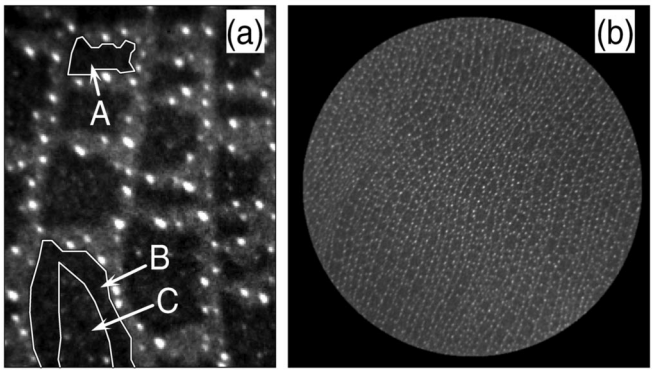

FIG. 5. Bright-field LEEM images taken after Ge deposition. (a) 945×1260 nm^2 detailed view. In the smaller Ga-depleted areas (e.g., region A), no Ge islands are found, in contrast to the larger ones (e.g., region B + C). The latter exhibit denuded zones (see region B) with a width of typically 90 nm. (b) Large-scale view (20 μm diameter), showing the alignment of Ge islands at step edges.

selective growth conditions observed here can be attributed to a locally surfactant-mediated epitaxy. It should be noted that in the presence of step bunches, a preferential nucleation of 3D islands has also been reported for the growth on bare Si(111) substrates [24,25]. However, such an alignment mechanism can be ruled out for the Ge islands on regularly stepped, bare Si(111) surfaces [25,26] as in the present case.

From a closer inspection of the LEEM images [see Fig. 5(a)], a kinetic limitation of the selective growth process becomes obvious. The 3D islands do not only nucleate at step edges and domain boundaries, but also start to evolve at the centers of the initial 7×7 domains. However, there are pronounced denuded zones at the borders of these domains. The width of the denuded zones, which can be interpreted as an effective diffusion length [13], is found to be about 90 nm for the growth conditions used here. Within the smallest of the initial 7×7 domains, virtually no 3D islands are found.

Finally, a large-scale view of the surface as shown in Fig. 5(b) clearly demonstrates the quality of alignment which can be achieved. Based on the present findings, a scheme for an even more pronounced island alignment may be deduced: for substrates with larger vicinality, the average terrace width becomes smaller. Hence, the initial 7×7 domain size can be made smaller than the denuded zone width. Therefore, such vicinal substrates could be applied in order to completely suppress the 3D island nucleation within the 7×7 domains and to tailor the size of the pattern. The approach of an adsorbate prepatterned surface may in principle also be applied to $Si_{1-x}Ge_x$ alloys. Superior to strain-based approaches, the pattern size could then be tuned independently of the chemical composition, leaving this parameter free for tailoring of the electronic properties.

In conclusion, we have demonstrated that a nanopatterned Si(111) surface can be achieved by high-temperature adsorption of Ga. We have also shown that these patterned substrates successively act as templates for selective nucleation and alignment of 3D Ge islands. In contrast to many other approaches, the underlying mechanism is not based on (volume) strain modulation, but on a modulation of surface properties. The results shown here open the door to a novel kind of nanostructure design, in which the structural and electronical properties may be tailored independently from each other.

We would like to acknowledge Wacker Siltronic for the kind supply of highly oriented Si wafers. This work has been supported by the European Community (Contract No. RII3-CT-2004-506008), and by the Deutsche Forschungsgemeinschaft (Grant No. FA 363/6).

*Present address: TASC-INFM Laboratory, Area di Ricerca, 34012 Basovizza, Italy.

[1] G. Abstreiter *et al.*, Semicond. Sci. Technol. **11**, 1521 (1996).
[2] J. Konle *et al.*, Solid-State Electron. **45**, 1921 (2001).
[3] A. Hirai and K. M. Itoh, Physica (Amsterdam) **E23**, 248 (2004).
[4] O. G. Schmidt *et al.*, Appl. Phys. Lett. **77**, 4139 (2000).
[5] Z. Zhong *et al.*, Physica (Amsterdam) **E23**, 243 (2004).
[6] A. Ronda and I. Berbezier, Physica (Amsterdam) **E23**, 370 (2004).
[7] E. V. Pedersen *et al.*, Surf. Sci. Lett. **399**, L351 (1998).
[8] J. Tersoff, C. Teichert, and M. G. Lagally, Phys. Rev. Lett. **76**, 1675 (1996).
[9] C. Teichert *et al.*, Phys. Rev. B **53**, 16334 (1996).
[10] K. Sakamoto *et al.*, Thin Solid Films **321**, 55 (1998).
[11] A. Portavoce *et al.*, Thin Solid Films **380**, 164 (2000).
[12] I. Berbezier, A. Ronda, A. Portavoce, and N. Motta, Appl. Phys. Lett. **83**, 4833 (2003).
[13] B. Voigtländer, A. Zinner, T. Weber, and H. P. Bonzel, Phys. Rev. B **51**, 7583 (1995).
[14] L. Simon *et al.*, Phys. Rev. B **64**, 035306 (2001).
[15] O. G. Schmidt *et al.*, Appl. Phys. Lett. **71**, 2340 (1997).
[16] D. Dentel *et al.*, J. Appl. Phys. **93**, 5069 (2003).
[17] J. Falta, M. Copel, F. K. LeGoues, and R. M. Tromp, Appl. Phys. Lett. **62**, 2962 (1993).
[18] T. Schmidt *et al.*, Surf. Rev. Lett. **5**, 1287 (1998).
[19] A. Locatelli *et al.*, J. Phys. IV (France) **104**, 99 (2003).
[20] Th. Schmidt *et al.*, New J. Phys. **7**, 193 (2005).
[21] J. Falta, Th. Schmidt, A. Hille, and G. Materlik, Phys. Rev. B **54**, R17288 (1996).
[22] R. M. Tromp and M. C. Reuter, Phys. Rev. B **47**, 7598 (1993).
[23] F. M. Ross, J. Tersoff, and R. M. Tromp, Phys. Rev. Lett. **80**, 984 (1998).
[24] H. Omi and T. Ogino, Thin Solid Films **369**, 88 (2000).
[25] A. Sgarlata *et al.*, Appl. Phys. Lett. **83**, 4002 (2003).
[26] B. Voigtländer and A. Zinner, Appl. Phys. Lett. **63**, 3055 (1993).